⌘ *Author's Choice*

THE JOURNAL OF BIOLOGICAL CHEMISTRY VOL. 287, NO. 6, pp. 4188–4197, February 3, 2012

Increased Angiogenesis Protects against Adipose Hypoxia and Fibrosis in Metabolic Disease-resistant 11β-Hydroxysteroid Dehydrogenase Type 1 (HSD1)-deficient Mice*[S]

Received for publication, May 13, 2011, and in revised form, December 8, 2011 Published, JBC Papers in Press, December 12, 2011, DOI 10.1074/jbc.M111.259325

Zoi Michailidou[‡1], Sophie Turban[§], Eileen Miller[§], Xiantong Zou[§], Joerg Schrader[‡], Peter J. Ratcliffe[¶], Patrick W. F. Hadoke[§], Brian R. Walker[§], John P. Iredale[‡], Nicholas M. Morton[§2], and Jonathan R. Seckl[§]

From the [‡]Medical Research Council (MRC) Centre for Inflammation Research and [§]University/British Heart Foundation (BHF) Centre for Cardiovascular Science, University of Edinburgh, Queen's Medical Research Institute, 47 Little France Crescent, Edinburgh EH16 4TJ, Scotland and the [¶]Nuffield Department of Clinical Medicine, University of Oxford, Henry Wellcome Building for Molecular Physiology, Roosevelt Drive, Oxford OX3 7BN, United Kingdom

Background: Adipose hypertrophy limits fat cell oxygenation, promotes scarring, and associates with increased local glucocorticoid regeneration (higher 11βHSD1 enzyme).
Results: 11βHSD1 knock-out mice have reduced scarring and better vascularization and oxygenation in their adipose tissue.
Conclusion: Elevated adipose 11βHSD1 contributes to obesity pathogenesis by suppressing adipose angiogenesis.
Significance: Enhancement of adipose oxygenation and vascularization is a novel therapeutic modality for 11βHSD1 inhibitors.

In obesity, rapidly expanding adipose tissue becomes hypoxic, precipitating inflammation, fibrosis, and insulin resistance. Compensatory angiogenesis may prevent these events. Mice lacking the intracellular glucocorticoid-amplifying enzyme 11β-hydroxysteroid dehydrogenase type 1 (11βHSD1$^{-/-}$) have "healthier" adipose tissue distribution and resist metabolic disease with diet-induced obesity. Here we show that adipose tissues of 11βHSD1$^{-/-}$ mice exhibit attenuated hypoxia, induction of hypoxia-inducible factor (HIF-1α) activation of the TGF-β/Smad3/α-smooth muscle actin (α-SMA) signaling pathway, and fibrogenesis despite similar fat accretion with diet-induced obesity. Moreover, augmented 11βHSD1$^{-/-}$ adipose tissue angiogenesis is associated with enhanced peroxisome proliferator-activated receptor γ (PPARγ)-inducible expression of the potent angiogenic factors VEGF-A, apelin, and angiopoietin-like protein 4. Improved adipose angiogenesis and reduced fibrosis provide a novel mechanism whereby suppression of intracellular glucocorticoid regeneration promotes safer fat expansion with weight gain.

In obesity, adipose tissue expansion may exceed compensatory vascular supply. Consequently, adipose tissue hypoxia is postulated to precipitate inflammatory macrophage infiltration and impair insulin signaling (1–4). Induction of hypoxia-inducible factors (HIFs)[3] is a molecular hallmark of tissue hypoxia. Both HIF-1α and HIF-2α are involved in adipocyte differentiation and responses to hypoxia *in vitro* (5, 6). HIF-1α associates with hypoxic and inflammatory changes in adipose tissues *in vivo*, and transgenic overexpression of HIF-1α in adipose tissue causes fibrosis (7).

Altered glucocorticoid action has a major impact upon adipose tissue distribution and insulin sensitivity. Elevated adipose tissue levels of the intracellular glucocorticoid-regenerating enzyme 11β-hydroxysteroid dehydrogenase type 1 (11βHSD1) are found in human obesity (8, 9). Modeling this by adipose-specific overexpression in mice drives visceral obesity and a metabolic syndrome (10). In contrast, 11βHSD1 gene knock-out (11βHSD1$^{-/-}$) mice are protected from high fat diet-induced metabolic disease (11, 12) and adipose inflammation (13). In addition, 11βHSD1 deficiency is associated with enhanced angiogenesis during wound healing and in the myocardium following ischemia (14, 15). We hypothesized that the metabolically "healthy" adipose tissue found with 11βHSD1 deficiency might have its origin in improved adipose tissue angiogenesis, with consequent improvement in hypoxia-induced fibrosis. We therefore examined the impact of 11βHSD1 deficiency on adipocyte paracrine, stromal proangiogenic responses, and the consequent effects on adipose tissue vascularization and fibrosis in dietary obesity.

* This work was supported by a Henry Wellcome Postdoctoral Fellowship (to Z. M.), a Wellcome Trust Programme Grant (to J. R. S.), and a grant from the European Community 7th Framework Programme (FP7/2007-2013) under Grant Agreement 201608, entitled Targeting Obesity-driven Inflammation (TOBI). B. R. W., J. R. S., and N. M. M. are inventors on relevant patents owned by the University of Edinburgh. B. R. W. and J. R. S. have consulted on 11βHSD1 inhibitors for a number of pharmaceutical companies.
⌘ *Author's Choice*—Final version full access.
[S] This article contains supplemental Figs. S1–S4.
[1] To whom correspondence should be addressed. Tel.: 44-131-2426670; E-mail: v1zmicha@staffmail.ed.ac.uk.
[2] Supported by a Wellcome Trust Career Development Fellowship (079660/z/06/z).

[3] The abbreviations used are: HIF, hypoxia-inducible factor; SVF, stromovascular fraction; ANGPTL4, angiopoietin protein-like 4; scAT, subcutaneous adipose tissue; mesAT, mesenteric adipose tissue; PHD, HIF prolyl hydroxylase; KO, 11βHSD1 knock-out; 11βHSD1, 11β-hydroxysteroid dehydrogenase type 1; DIO, diet-induced obesity; PPAR, peroxisome proliferator-activated receptor; HF, high fat; α-SMA, α-smooth muscle actin; ANOVA, analysis of variance; Bis-Tris, 2-(bis(2-hydroxyethyl)amino)-2-(hydroxymethyl)propane-1,3-diol.

TABLE 1

Similar body weight and adipose mass gain in 11βHSD1$^{-/-}$ mice after HF feeding

11βHSD1$^{-/-}$ and control (C57BL/6) mice gained similar weight ($n = 6$). Body fat distribution and subcutaneous and mesenteric fat deposition were similar after 12 weeks on HF diet. * indicates significant differences between control chow and high fat diet in both genotypes. CD, chow-fed; HFD, high fat diet-fed; BW, body weight.

	C57BL/6 CD	C57BL/6 HFD	11βHSD1$^{-/-}$ HFD	*p* values
Terminal BW (g)	38.8 ± 3.2*	49.2 ± 1.7	53 ± 1.1	<0.0001
BW gain (g)	5.9 ± 0.3*	16.1 ± 1.2	17.1 ± 1.2	<0.0001
scAT (g)	0.4 ± 0.03*	1.0 ± 0.06	1.2 ± 0.09	<0.0001
mesAT (g)	0.7 ± 0.06*	1.5 ± 0.1	1.6 ± 0.1	<0.0001
scAT/BW ratio	0.010 ± 0.0006*	0.020 ± 0.001	0.022 ± 0.001	<0.0001
mesAT/BW ratio	0.018 ± 0.0009*	0.030 ± 0.001	0.031 ± 0.001	0.0006

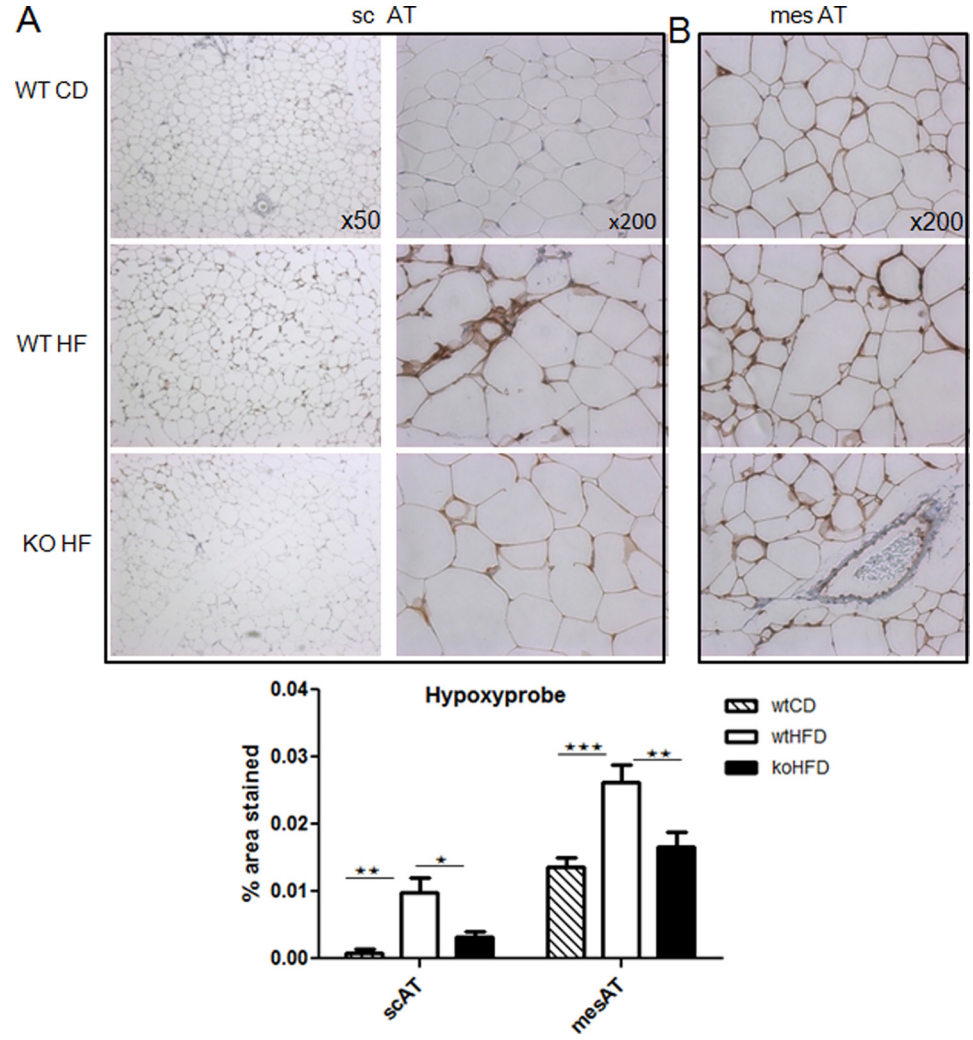

FIGURE 1. **Less adipose hypoxia in 11βHSD1$^{-/-}$ mice.** *A* and B, representative images of Hypoxyprobe staining of subcutaneous (*A*) and mesenteric (*B*) adipose tissue in chow-fed control (*WT CD*; quantification histogram: *hatched bars*), HF-fed control (*WT HF*; quantification histogram: *white bars*), and HF 11βHSD1$^{-/-}$ (*KO HF*; quantification histogram: *black bars*) mice ($n = 6$). 30–40 high power fields (magnification ×200) per section were quantified. *Brown adducts* indicate areas of low oxygen availability. Note the unstained blood vessel that acts as an internal negative control. $n = 6$/group, *, $p < 0.05$, **, $p < 0.01$,***, $p < 0.001$ by ANOVA. *HFD*, high fat diet.

EXPERIMENTAL PROCEDURES

Diet-induced Obesity (DIO)—Adult male 11βHSD1$^{-/-}$ and congenic C57Bl/6J controls (12, 13) were single-housed (12-h light/12-h dark cycle) and given food and water *ad libitum*. Mice ($n = 6–8$ per group) were randomized to standard chow or a high fat (HF) diet, 58% calories as fat (Research Diets D12331), for 12 weeks.

Pimonidazole Staining—To assess adipose tissue hypoxia *in vivo*, mice were injected intraperitoneally with 60 mg/kg of pimonidazole (Hypoxyprobe^{TM}-1 Plus kit, Chemicon International), 30 min prior to sacrifice. Subcutaneous (scAT) and mesenteric (mesAT) adipose tissues were collected in formalin and paraffin-embedded. 4-μm sections were incubated with mAb1 conjugated with FITC at a 1:100 dilution for 30 min at room temperature. A secondary anti-FITC mAb was applied at a 1:100 dilution for 30 min (according to the manufacturer's instructions). Pimonidazole adduct staining was visualized using the diaminobenzidine chromogen-A system (DAKO). Sections were rinsed and counterstained with hematoxylin and imaged using a Zeiss microscope. 30–40 high power fields

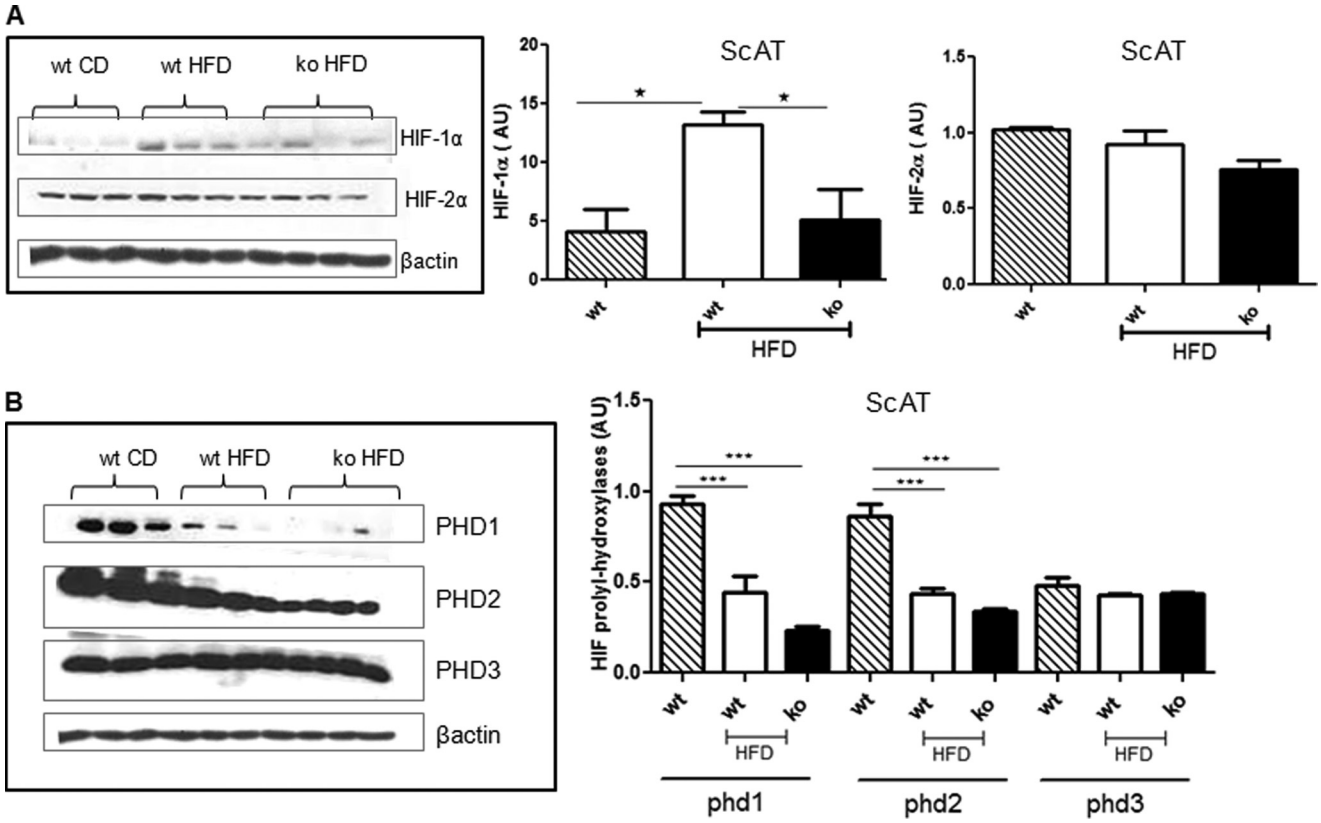

FIGURE 2. **Reduced adipose HIF-1α in 11βHSD1$^{-/-}$ mice.** *A* and *B*, representative immunoblots of HIF-1α and HIF-2α protein levels (*A*) and PHD 1–3 protein levels (*B*) in scAT. *Right panels*, quantification histograms showing the relative protein levels corrected for β-actin control mice on chow diet (*hatched bars*, $n = 6$), control HF (*white bars*, $n = 6$), and 11βHSD1$^{-/-}$ HF mice (*black bars*, $n = 6$). *, $p < 0.05$, ***, $p < 0.001$ by ANOVA. *AU*, arbitrary units; *WT CD*, chow-fed control; *wt HFD*, HF-fed control; *KO HFD*, HF 11βHSD1$^{-/-}$.

(magnification ×200) per section were randomly selected for each slide by an assessor blind to genotype. Diaminobenzidine brown staining was quantified using Photoshop PS3 and normalized to the total number of pixels.

RNA Extraction and Quantitative Real Time PCR—scAT and mesAT were weighed and snap-frozen in liquid nitrogen, and RNA was extracted as described (12). 1 μg of RNA was reverse-transcribed using the SuperScript III cDNA synthesis kit (Invitrogen) according to the manufacturer's instructions. Real time PCR was performed with the LightCycler (Roche Applied Science), using TaqMan assays for all genes measured and correcting for 18 S and β-actin expression.

Immunoblotting—Frozen adipose tissues were homogenized in a urea/SDS buffer supplemented with Complete protease inhibitor (Roche Applied Science). The fat layer was removed by centrifugation (4000 rpm, 10 min). The protein concentration was determined using a Bio-Rad assay kit. Proteins were separated on 7–12% Bis-Tris gels and transferred to PVDF membranes (Millipore). The antibodies used were rabbit anti-mouse HIF-1α, HIF-2α, PHD2, PHD1, PHD3 (Novus Biologicals), anti-phospho-Smad3 (Cell Signaling), anti-Smad2/3 (Cell Signaling), anti-α-SMA (Sigma), and HRP-conjugated anti-β-actin (Abcam). The primary antibodies were detected with secondary HRP-IgGs (Dako) using ECL detection (GE Healthcare). Densitometry was performed using ImageJ, and protein levels were corrected for β-actin.

Immunohistochemistry—For the detection of collagen deposition, formalin-fixed, paraffin-embedded sections (4 μm) were stained with picrosirius red (Sigma). Myofibroblasts were detected with a mouse monoclonal antibody to α-SMA (Sigma). An anti-CD31 antibody (Abcam) was used for identifying endothelial cells/vessels. Secondary antibodies were all from Dako. Binding of primary antibody was visualized using diaminobenzidine chromogen-A (Dako) after counterstaining with hematoxylin.

SVF Cell Preparation and in Vitro Hypoxia—Adipose tissue was removed from HF-fed mice into warmed Krebs' buffer and collagenase type 1 (Worthington Biochemicals)-digested as described (30). Briefly, after 1 h of digestion and centrifugation to separate from adipocytes, stromovascular fraction (SVF) cells were seeded at 2.5×10^5 cells/well in DMEM. On day 2, culture medium was replaced with 1% O_2 preconditioned medium. Cells were left at 1% O_2 in a hypoxic chamber (1% O_2) for 6 h and then lysed in TRIzol, and RNA was extracted as above.

Rosiglitazone Treatment of Primary Adipocytes—The ceiling-cultured adipocytes from collagenase digestion (see above) were filtered through a 200-μm size exclusion mesh and then centrifuged. Equal volumes of fractionated adipocytes were cultured in DMEM medium (Lonza, Berkshire, UK) for 16 h at 37 °C, 5% CO_2 in the presence or absence of 1 μM rosiglitazone. Adipocytes were lysed in TRIzol, and total RNA was extracted as above.

Angiogenesis Bioassays—Strips of periaortic adipose tissue (immediately adjacent to the adventitia) were isolated from the thoracic aortas of C57Bl/6 or 11βHSD1$^{-/-}$ mice and incubated

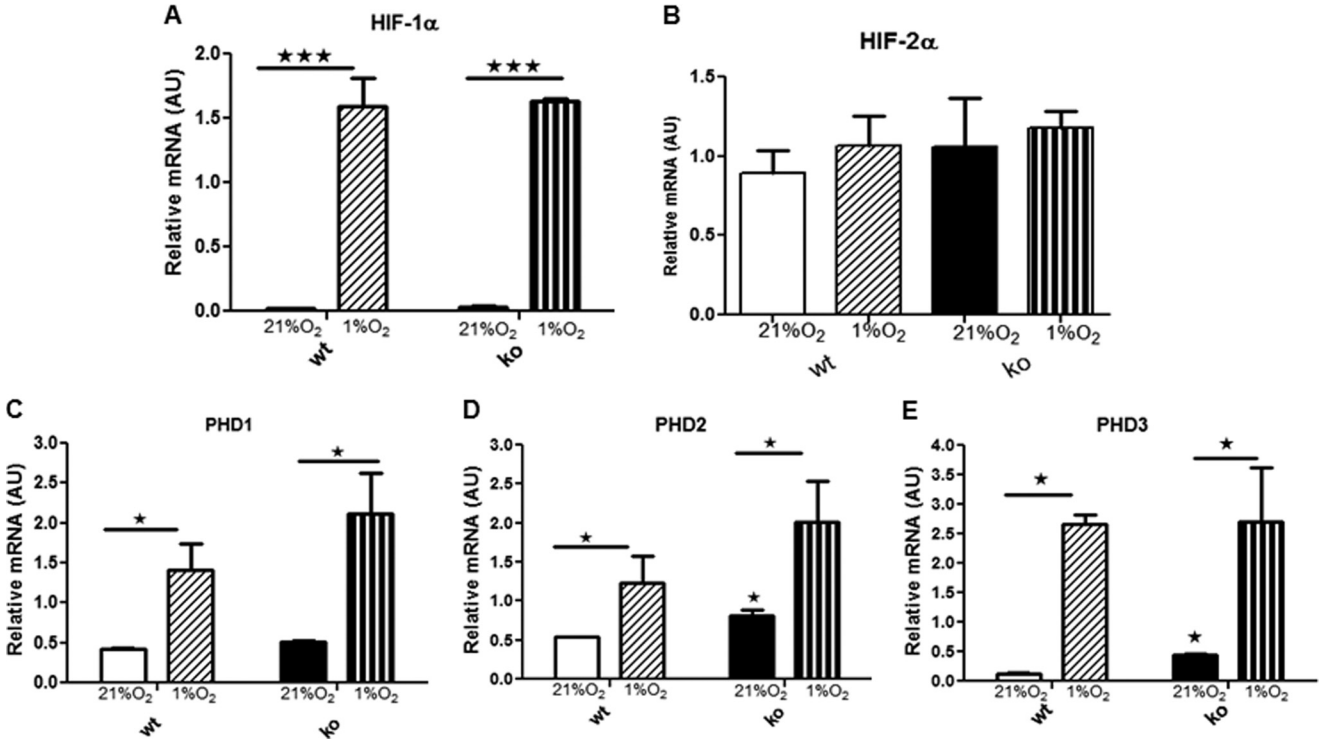

FIGURE 3. **11βHSD1$^{-/-}$ show similar HIF response after acute hypoxia *in vitro*.** *A–E*, SVF from HF control at 21% oxygen (*white*) and 1% oxygen (*diagonal hatched*) and HF 11βHSD1$^{-/-}$ at 21% oxygen (*black*) and 1% oxygen (*vertical hatched*). Cells were kept in 1% oxygen for 6 h. Data are presented as means ± S.E. of SVF from four individual mice. mRNA levels of HIF-1α (*A*), HIF-2α (*B*), PHD1 (*C*), PHD2 (*D*), and PHD3 (*E*) were determined. *, $p < 0.05$, ***, $p < 0.001$, by two-way ANOVA. *AU*, arbitrary units.

(20 mg of periaortic adipose/ml; 24 h at 37 °C) in DMEM containing 4.5 g/liter glucose, 584 mg/liter L-glutamine, 75 mg/liter L-ascorbic acid, 10 mg/liter heparin, 100 units/ml penicillin, 100 μg/ml streptomycin, 250 ng/ml amphotericin B, and 0.2% BSA. Adipose tissue was removed from the conditioned medium, which was aliquoted and stored at −80 °C. Control medium (vehicle) was obtained following the same procedure without adipose tissue. Tube formation from mouse aortic rings was performed as described (14). Briefly, aortic rings (~1 mm in length) from C57Bl/6 mice were embedded in Matrigel and incubated (DMEM, 37 °C; 5% CO_2) in 50% DMEM; 50% periaortic fat conditioned medium or 50% DMEM; 50% control medium for 7 days, with medium refreshed every 48 h. Aortic rings cultured under these conditions in Matrigel spontaneously generated endothelial tube-like structures. The impact of periaortic fat conditioned medium on angiogenesis was quantified by counting the number of tube-like structures every other day (by an operator blinded to treatment).

Statistical Analysis—Values are means ± S.E. Simple comparisons were analyzed using Student's *t* test. For multiple comparisons, differences between genotypes and the effect of treatment(s) were analyzed by two-way ANOVA with subsequent Tukey's post hoc test. Significance was set at $p < 0.05$.

RESULTS

11βHSD1$^{-/-}$ Adipose Tissue Is Resistant to Hypoxia with Obesity—Weight gain and fat mass were similar after 12 weeks of HF feeding in both genotypes (Table 1). This intermediate time point suggests that a convergent phase in fat accumulation follows an earlier generalized reduction in fat mass (13) and precedes a later beneficial redistribution of fat away from visceral depots and into peripheral fat depots (12).

Despite similar scAT depot expansion in 12-week HF-fed 11βHSD1$^{-/-}$ mice, there was markedly less adipose tissue pimonidazole staining and hence hypoxia than in HF-fed control (WT) mice (Fig. 1). Importantly, mesAT from chow-fed animals exhibited 14-fold ($p = 0.005$) greater pimonidazole staining than scAT, suggesting that marked hypoxia occurs under basal circumstances in this depot. HF feeding significantly induced adipose HIF-1α in control mice, whereas HIF-1α remained very low in similarly obese HF-fed 11βHSD1$^{-/-}$ mice (Fig. 2*A* and supplemental Fig. S1). HIF-2α protein was unaffected by HF or 11βHSD1 genotype (Fig. 2*A*), suggesting that it does not play a role in adipose hypoxic responses *in vivo*.

HIF prolyl hydroxylases (PHD 1–3 (also known as EGLNs)) degrade HIFs under normoxic conditions by hydroxylation of the two proline residues in the oxygen-dependent degradation domain of HIF-α (16–18). The role of PHDs in adipose tissue and obesity is currently unknown. Adipose tissue PHD mRNAs were unaffected by HF feeding or genotype (supplemental Fig. S2). However, PHD1 and PHD2 protein levels were suppressed by HF feeding (Fig. 2*B*). Thus, although lower PHD1 and PHD2 (and hence reduced HIF-1α degradation) may contribute to HIF-1α elevation with DIO in controls, variation in PHDs does not explain the lower levels of HIF-1α in adipose tissue with 11βHSD1 deletion.

To determine whether 11βHSD1$^{-/-}$ mice have altered responses to hypoxia in the fibrogenic adipose SVF, HIFs and

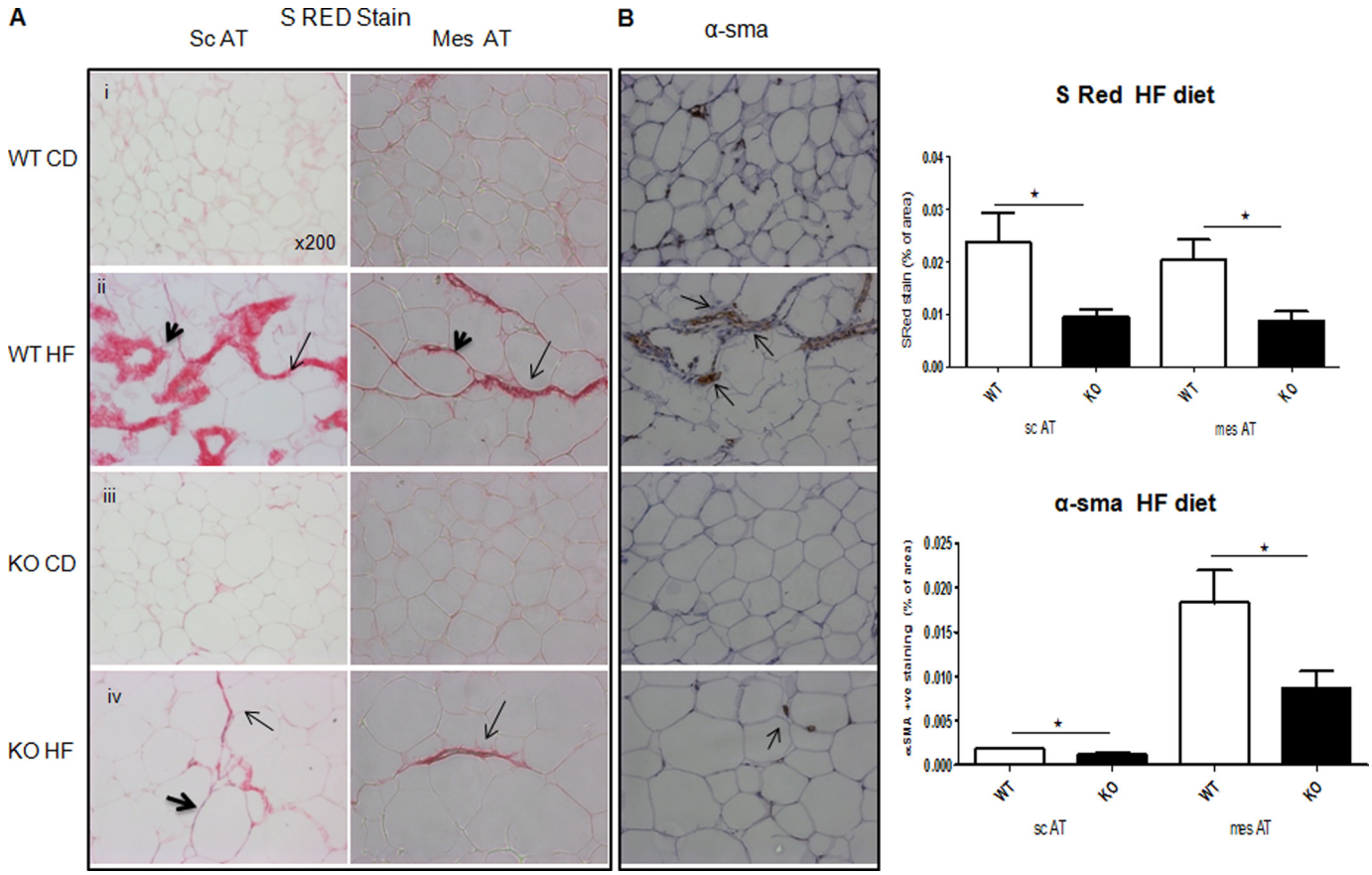

FIGURE 4. **Attenuated adipose tissue fibrosis in HF 11βHSD1$^{-/-}$.** *A*, representative images of picrosirius red (*S RED*) staining in subcutaneous (*sc*) and mesenteric (*mes*) adipose. *Bold arrowheads* show collagen deposition surrounding the adipocytes, and *arrows* point to the streaks of collagen between adipocytes. *WT CD*, chow-fed control; *wt HF*, HF-fed control; *KO CD*, chow-fed 11βHSD1$^{-/-}$; *KO HF*, HF 11βHSD1$^{-/-}$. *B*, α-SMA immunohistochemistry in mesenteric adipose; brown stained myofibroblasts are indicated by *arrows*. 30–40 fields (magnification ×200) per section were assessed in each group. *Right*, quantification histograms ($n = 6$/genotype) showing WT HF (*white bars*) *versus* KO HF (*black bars*) *, $p < 0.05$.

PHDs were measured in SVF cells from HF-fed mice under normoxia (21% O_2) or acute hypoxia (1% O_2) *in vitro*. In both genotypes, HIF-1α, but not HIF-2α, mRNA levels were markedly and similarly up-regulated by hypoxia (Fig. 3, *A* and *B*). All three PHDs were expressed in SVF cells and were similarly up-regulated by hypoxia (Fig. 3, *C–E*). Thus, the attenuation of HIF-1α responses to HF in 11βHSD1$^{-/-}$ adipose tissue *in vivo* is likely due to the reduced tissue hypoxia rather than an intrinsic difference in hypoxia responses.

HF-fed 11βHSD1$^{-/-}$ Mice Have Reduced Adipose Collagen Deposition and Expression of Fibrogenic Mediators—To determine whether obesity-induced hypoxia impacted adipose fibrosis, as in liver (19), we analyzed collagen deposition. Staining for picrosirius red-reactive collagens I and III was low and comparable between genotypes in chow-fed scAT and mesAT. HF diet markedly induced collagen staining in adipose tissue, observed as broad strands transversing the tissue and around individual adipocytes (Fig. 4*A*). 11βHSD1$^{-/-}$ mice exhibited significantly less collagen deposition in response to HF in both fat depots with much thinner fibrillar streaks and little staining around adipocytes (Fig. 4*A*).

Tissue fibrosis is characterized by increased transdifferentiation of fibroblasts to activated myofibroblasts and collagen deposition (20). 11βHSD1$^{-/-}$ adipose tissue exhibited reduced α-SMA staining in both scAT and mesAT adipose in response to HF (Fig. 4*B*). Consistent with reduced fibrosis and fewer α-SMA-positive cells, glucocorticoid-regulated Col1α1 mRNA levels were lower in 11βHSD1$^{-/-}$ adipose tissue (Fig. 5*C*). Other genes involved in fibrosis were unaltered in HF-fed 11βHSD1$^{-/-}$ adipose tissues, including Col3α1 and Col6α1 (Fig. 5*C*). Activation of the TGF-β/Smad signaling pathway is critical in driving fibrogenesis in liver (21) and in adipose tissue (7). To investigate the impact of intra-adipose glucocorticoid deficiency on adipose fibrosis, we measured TGF-β/Smad signaling. TGF-β mRNA (Fig. 5*C*) and total Smad2/3 (Fig. 5*A*) levels were comparable across genotypes and diet. HF feeding significantly induced Smad3 phosphorylation in control mice (3-fold, $p < 0.01$, Fig. 5*A* and supplemental Fig. S3). However, Smad3 phosphorylation levels were lower in HF-fed 11βHSD1$^{-/-}$ (Fig. 5*A*). *In vitro* hypoxia rapidly up-regulated TGF-β in SVF cells from control mice, whereas TGF-β was unchanged in 11βHSD1$^{-/-}$ SVF cells (supplemental Fig. S4). Moreover, the fibrosis-associated 63-kDa MMP14 pro-enzyme was elevated by HF diet in adipose tissue of control but not 11βHSD1$^{-/-}$ mice (Fig. 5*B*). Other matrix remodeling enzymes were unaltered including TIMP-1, MMP2, and MMP13 mRNA levels (Fig. 5*C*).

Increased Angiogenesis in 11βHSD1$^{-/-}$ Adipose Tissue—We next explored whether the attenuation of adipose tissue hypoxia and fibrosis responses in HF-fed 11βHSD1$^{-/-}$ adipose

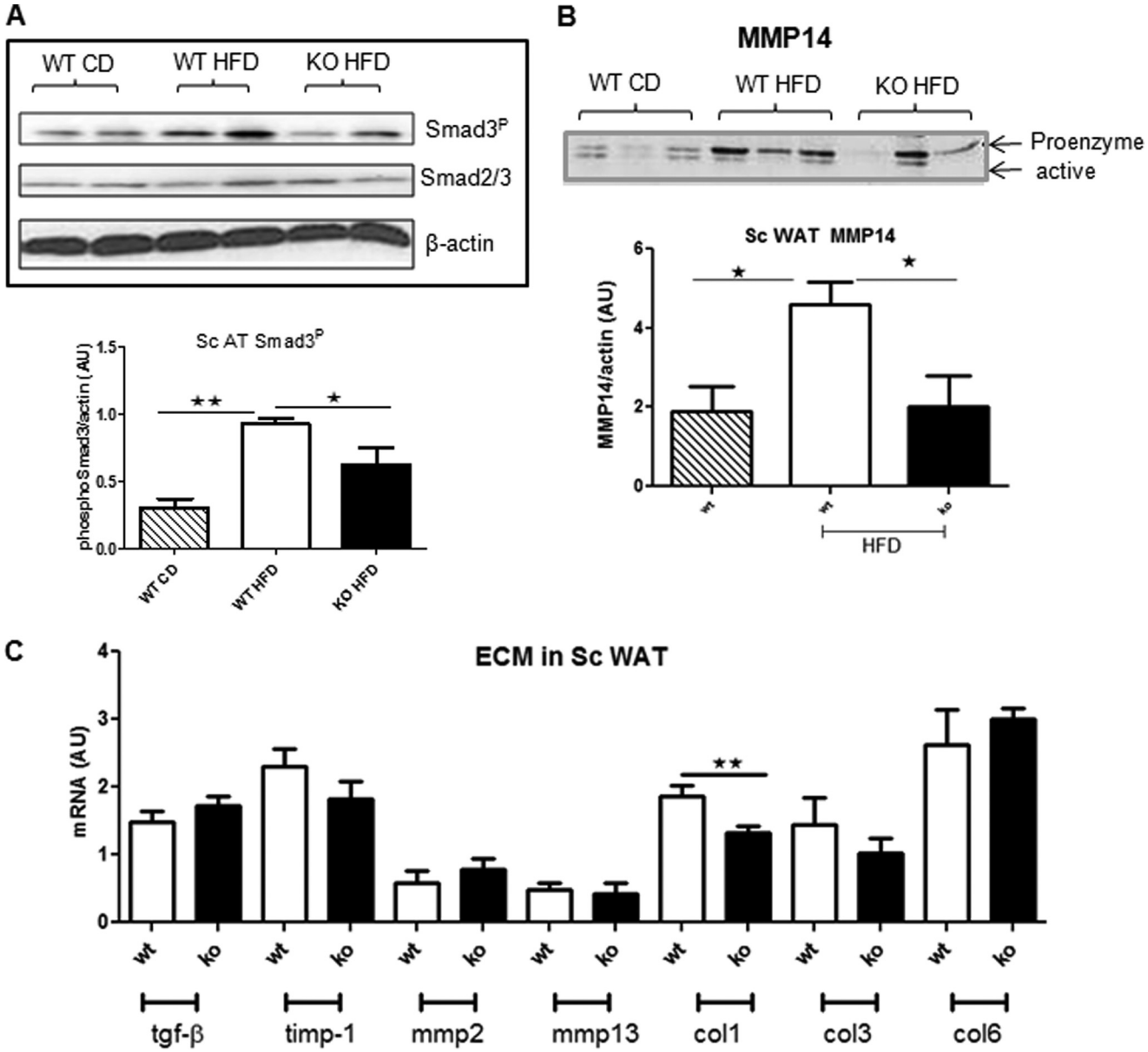

FIGURE 5. **Reduced profibrotic signaling in 11βHSD1$^{-/-}$.** *A* and *B*, representative adipose Western blots of phosphorylated Smad3 (*Smad3^{P}*) (*A*) and unphosphorylated Smad2/3 protein pro-enzyme and active MMP14 (*B*). *Lower panels*, protein quantification histograms for control mice on chow diet (*WT CD*, *hatched bars*, $n = 4$), control HF (*WT HFD*, *white bars*, $n = 4$), and 11βHSD1$^{-/-}$ HF mice (*KO HFD*, *black bars*, $n = 4$). *AU*, arbitrary units. *C*, mRNA of a panel of profibrotic genes ($n = 8$/genotype). *White* and *black bars*, differences between control on HF (*white bars*) and 11βHSD1$^{-/-}$ on HF (*black bars*) by Student's *t* test. *, $p < 0.05$, **, $p < 0.01$.

tissues was associated with enhanced angiogenesis. The vessel-to-adipocyte ratio (correcting for adipose hypertrophy) was higher in HF-fed 11βHSD1$^{-/-}$ mice than in control mice (Fig. 6*A*) despite comparable reductions in total vessel (Fig. 6*B*) and fat cell numbers (Fig. 6*C*). This appeared to be a direct effect of 11βHSD1$^{-/-}$ adipose tissue on functional induction of angiogenesis because exposure of control aortic rings to 11βHSD1$^{-/-}$ adipose tissue-conditioned medium induced greater angiogenesis (3-fold, $p < 0.01$) than control (1.5-fold, $p < 0.05$) adipose tissue medium (Fig. 7).

To explore the potential adipose tissue factors involved, we measured key angiogenic gene expression levels. VEGF-A, ANGPTL4, and apelin mRNA were more highly expressed in adipose tissue of 11βHSD1$^{-/-}$ than in control mice (Fig. 8*A*). SVF endothelial cells are key to adipose tissue expansion (22). Consistent with the *in vivo* findings, normoxic SVF cells from 11βHSD1$^{-/-}$ adipose tissue had higher VEGF-A and ANGPTL4 expression (Fig. 8, *B* and *C*). Hypoxia induced SVF cell VEGF-A and ANGPTL4 mRNA expression to a greater extent in 11βHSD1$^{-/-}$ (Fig. 8*B*).

To determine whether the increased PPARγ sensitivity of 11βHSD1$^{-/-}$ adipocytes (13) might contribute in a paracrine manner to enhanced SVF angiogenic responses, primary mesAT adipocytes from HF-fed mice were treated with the PPARγ agonist rosiglitazone (1 μM) for 24 h. As *in vivo*, ANGPTL4 (although not VEGF) was more highly expressed in 11βHSD1$^{-/-}$ adipocytes *in vitro* (Fig. 9*B*). Rosiglitazone up-regulated adipose ANGPTL4 with a 2-fold greater effect in

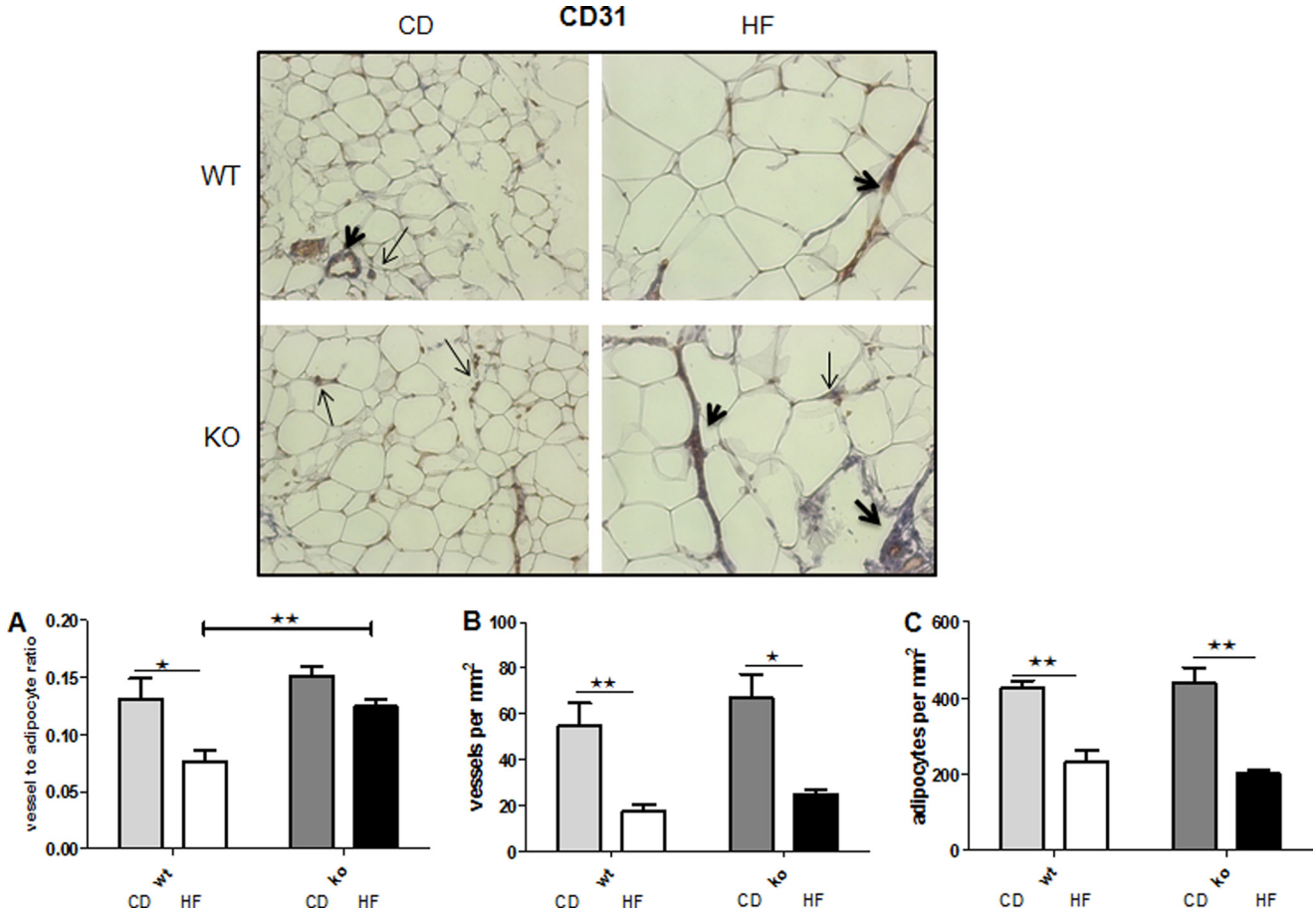

FIGURE 6. **Higher vessel-to-adipocyte ratio in 11βHSD1$^{-/-}$ in obesity.** *Top panels*, representative pictures (×200 magnification) showing vessel staining using a CD31 antibody. *Arrows* indicate individual CD31-positive cells, and *bold arrowheads* indicate stained vessels. 30–40 fields per section were randomly selected, and the number of vessels positively staining for CD31 normalized to the total number of adipocytes was quantified blind to genotype. *CD*, chow-fed. *A–C*, quantification of total vessels to adipocyte ratio (*A*), total vessel number per area (mm^2) (*B*), and total adipocyte number per area (mm^2) (*C*). $n = 4$, *, $p < 0.05$, **, $p < 0.01$.

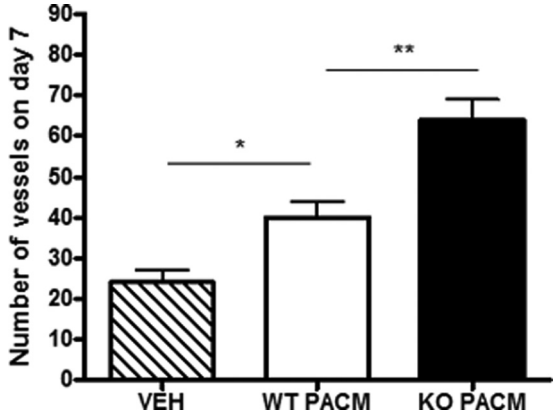

FIGURE 7. **Higher capacity of adipose-mediated tube-like structure formation in 11βHSD1$^{-/-}$ mice.** The number of tube-like structures formed from mouse aortic rings after the addition of vehicle (*VEH*, *hatched bars*), wild type periaortic fat conditioned media (*WT PACM*, *white bars*), or 11βHSD1$^{-/-}$ periaortic fat conditioned media (*KO PACM*, *black bars*) was assessed. $n = 4$, *, $p < 0.05$, **, $p < 0.01$.

11βHSD1$^{-/-}$ adipocytes. VEGF-A was induced by rosiglitazone in 11βHSD1$^{-/-}$ but not control adipocytes (Fig. 9*A*).

DISCUSSION

Here we show that relative glucocorticoid deficiency within adipose tissue is permissive for angiogenesis in response to DIO, thus preventing severe hypoxia and consequent inflammation, metabolic dysfunction, and fibrosis. We find that DIO induces more severe hypoxia in mesenteric AT than in subcutaneous AT. This is associated with HIF-1α induction through reduced PHD1- and PHD2-mediated HIF degradation. This cascade of responses associates with induction of TGF-β/Smad/α-SMA signaling, myofibroblast activation, increased collagen deposition, and MMP14 induction in HF-fed C57BL/6J but not 11βHSD1$^{-/-}$ mice. Increased PPARγ activation and induction of adipocyte angiogenic factors associates with the improved 11βHSD1$^{-/-}$ adipose tissue phenotype. This work suggests that a cascade of failed angiogenesis leads to tissue hypoxia and fibrosis in rapidly expanding adipose tissue in obesity. This is ameliorated with intra-adipose glucocorticoid deficiency.

Adipose tissue hypoxia mediates insulin resistance and inflammation in obesity (1–4). Moreover, hypoxia is profibrotic in adipose tissue, with transgenic overexpression of adipose-HIF-1α leading to exacerbated collagen deposition and fibrosis (7). Although persistent inflammation precedes fibrosis (23), it is unclear whether chronic low grade inflammation of obesity alters angiogenesis-dependent hypoxia and consequent adipose tissue fibrosis. Loss of the potent angiogenic factor VEGF in myeloid cells leads to excessive collagen deposition

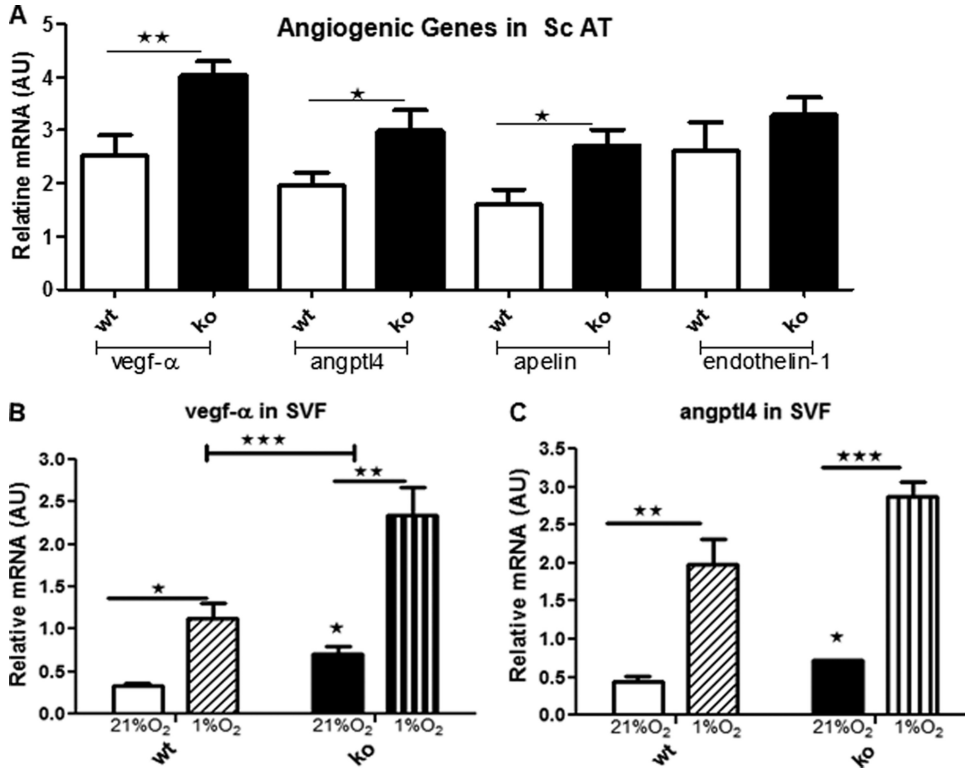

FIGURE 8. **Higher expression of proangiogenic genes in 11βHSD1$^{-/-}$ in obesity.** *A*, adipose mRNA levels of a panel of potent angiogenic factors, corrected for β-actin ($n = 8$). The bars indicate the following: SVF from HF control at 21% oxygen (*white bars*), 1% oxygen (*diagonal hatched bars*), HF 11βHSD1$^{-/-}$ 21% oxygen (*black bars*) and 1% oxygen (*vertical hatched bars*). Cells were kept in 1% oxygen for 6 h. Data are presented as means ± S.E. SVF was prepared from four individual mice. *AU*, arbitrary units. *B* and *C*, mRNA levels of VEGF-A (*B*) and ANGPTL4 (*C*). *, $p < 0.05$, **, $p < 0.01$, and ***, $p < 0.001$.

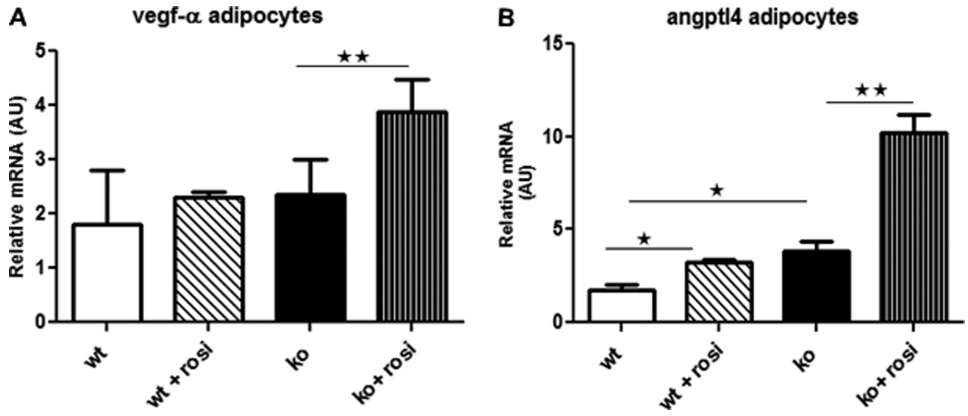

FIGURE 9. **11βHSD1$^{-/-}$ adipocytes are more sensitive to PPARγ-mediated angiogenic gene induction.** *A* and *B*, VEGF-A (*A*) and ANGPTL4 (*B*) mRNA levels in adipocytes from HF-fed control mice (*white bars*, $n = 4$), rosiglitazone-treated mice (*diagonal hatched bars*, $n = 6$), 11βHSD1$^{-/-}$-untreated mice (*black bars*, $n = 4$) and rosiglitazone-treated mice (*vertical hatched bars*, $n = 6$). Two-way ANOVA, *, $p < 0.05$, **, $p < 0.01$. *AU*, arbitrary units.

and fibrosis, indicating that inflammatory cell-derived VEGF is required for vascular remodeling (24). Failure of extracellular matrix remodeling and/or neovascularization during adipose expansion could feasibly lead to adipose tissue fibrosis. Indeed, genetically obese mice and obese humans show significantly reduced adipose VEGF-A accompanied by lower capillary density (4, 25), suggesting reduced adaptive angiogenesis. Although hypoxia up-regulates VEGF-A, the protective angiogenic response observed in 11βHSD1$^{-/-}$ mice did not follow the canonical hypoxia-HIF-dependent pathway. HIF-independent regulation of VEGF-A and angiogenesis through PPARγ coactivator PGC-1α-mediated responses occurs in skeletal muscle (26) and brain (27). Moreover, induction of HIF-1α in DIO or adipose HIF-1α overexpression does not increase VEGF-A (7). Glucocorticoids potently suppress angiogenesis through inhibition of VEGF-A (28, 29). Consistent with this, reduced hypoxia and fibrosis in adipose tissue from 11βHSD1$^{-/-}$ mice showed augmented PPARγ activation that is associated with induction of adipocyte VEGF-A and ANGPLT4 and sustained vessel density. Moreover, the SVF cells (fibroblast/endothelial population) are more responsive to DIO-mediated hypoxia in 11βHSD1$^{-/-}$ mice, driving beneficial adipose tissue remodeling. 11βHSD1 is highly expressed in the fibroblastic preadipocytes (30) and not the SVF macrophages (13), suggesting that

$11\beta HSD1^{-/-}$ preadipocytes and/or endothelial cells likely mediate the beneficial response to hypoxia/inflammation and fibrosis associated with obesity.

Distinct adipose depots exhibited different degrees of hypoxia, under basal or obesogenic conditions. Thus, mesAT is more hypoxic as compared with scAT depot. This suggests that hypoxia does not progress uniformly between depots, most probably due to differences in the initial degree of depot vascularization or in the rate/capacity of neovascularization during expansion. This is consistent with greater capillary density and angiogenic capacity in human subcutaneous *versus* visceral adipose tissue (25, 31). This suggests that individuals prone to visceral fat accumulation are at higher risk of hypoxia-induced metabolic dysfunction. Our finding that glucocorticoid deficiency is associated with fewer hypoxic areas, and consequently normoxic HIF-1α levels, in both depots, in contrast to what is seen in DIO or genetically obese mice (1, 32), suggests a metabolic/vascular advantage during adipose expansion. Glucocorticoids could exacerbate the induction of HIF-1α-dependent gene expression under hypoxic conditions and enhance the hypoxic metabolic insult (29, 33). Importantly, our data suggest that HIF-1α might be regulated (stabilized/activated) by other pathway(s) apart from tissue hypoxia *per se* during obesity such as inflammatory cytokines (34, 35) and insulin (36–38) pathways. In agreement with this, HF-fed $11\beta HSD1^{-/-}$ mice are insulin-sensitized and have reduced adipose inflammation (12, 13).

We propose that increased local glucocorticoid amplification exacerbates the metabolic insult caused by hypoxia and consequent fibrosis in adipose tissue. The detrimental impact on adipose tissue architecture may then lead to further metabolic compromise of adipocytes. Thus, selective 11βHSD1 inhibition might prove to be beneficial both by increasing adipocyte insulin sensitivity and function and by favoring enhanced angiogenesis signals, allowing escape from adipose hypoxia and fibrosis in obesity.

Acknowledgments—We acknowledge the support of the British Heart Foundation Centre of Research Excellence. We are grateful to the Centre for Inflammation Research Histology staff for excellent technical support and Sheila Macpherson in the MRC-Centre for Reproductive Biology (CRB) for expertise and generous help on CD31 immunohistochemistry.

REFERENCES

1. Hosogai, N., Fukuhara, A., Oshima, K., Miyata, Y., Tanaka, S., Segawa, K., Furukawa, S., Tochino, Y., Komuro, R., Matsuda, M., and Shimomura, I. (2007) Adipose tissue hypoxia in obesity and its impact on adipocytokine dysregulation. *Diabetes* **56,** 901–911
2. Rausch, M. E. Weisberg, S., Vardhana, P., and Tortoriello, D. V. (2008) Obesity in C57BL/6J mice is characterized by adipose tissue hypoxia and cytotoxic T-cell infiltration. *Int. J. Obes. (Lon.)* **32,** 451–463
3. Yin, J., Gao, Z., He, Q., Zhou, D., Guo, Z., and Ye, J. (2009) Role of hypoxia in obesity-induced disorders of glucose and lipid metabolism in adipose tissue. *Am. J. Physiol. Endocrinol. Metab.* **296,** E333–E342
4. Pasarica, M., Sereda, O. R., Redman, L. M., Albarado, D. C., Hymel, D. T., Roan, L. E., Rood, J. C., Burk, D. H., and Smith, S. R. (2009) Reduced adipose tissue oxygenation in human obesity: evidence for rarefaction, macrophage chemotaxis, and inflammation without an angiogenic response. *Diabetes* **58,** 718–725
5. Yun, Z., Maecker, H. L., Johnson, R. S., and Giaccia, A. J. (2002) Inhibition of *PPARγ2* gene expression by the HIF-1-regulated gene *DEC1/Stra13*: a mechanism for regulation of adipogenesis by hypoxia. *Dev. Cell* **2,** 331–341
6. Shimba, S., Wada, T., Hara, S., Tezuka, M. (2004) EPAS1 promotes adipose differentiation in 3T3-L1 cells. *J. Biol. Chem.* **279,** 40946–40953
7. Halberg, N., Khan, T., Trujillo, M. E., Wernstedt-Asterholm, I., Attie, A. D., Sherwani, S., Wang, Z. V., Landskroner-Eiger, S., Dineen, S., Magalang, U. J., Brekken, R. A., and Scherer, P. E. (2009) Hypoxia-inducible factor 1α induces fibrosis and insulin resistance in white adipose tissue. *Molecular and cellular biology* **29,** 4467–4483
8. Rask, E., Olsson, T., Söderberg, S., Andrew, R., Livingstone, D. E., Johnson, O., Walker, B. R. (2001) Tissue-specific dysregulation of cortisol metabolism in human obesity. *J. Clin. Endocrinol. Metab.* **86,** 1418–1421
9. Michailidou, Z., Jensen, M. D., Dumesic, D. A., Chapman, K. E., Seckl, J. R., Walker, B. R., and Morton, N. M (2007) Omental 11β-hydroxysteroid dehydrogenase 1 correlates with fat cell size independently of obesity. *Obesity* **15,** 1155–1163
10. Masuzaki, H., Paterson, J., Shinyama, H., Morton, N. M., Mullins, J. J., Seckl, J. R., and Flier, J. S. (2001) A transgenic model of visceral obesity and the metabolic syndrome. *Science* **294,** 2166–2170
11. Kotelevtsev, Y., Holmes, M. C., Burchell, A., Houston, P. M., Schmoll, D., Jamieson, P., Best, R., Brown, R., Edwards, C. R., Seckl, J. R., and Mullins, J. J. (1997) 11β-hydroxysteroid dehydrogenase type 1 knockout mice show attenuated glucocorticoid-inducible responses and resist hyperglycemia on obesity or stress. *Proc. Natl. Acad. Sci. U.S.A.* **94,** 14924–14929
12. Morton, N. M., Paterson, J. M., Masuzaki, H., Holmes, M. C., Staels, B., Fievet, C., Walker, B. R., Flier, J. S., Mullins, J. J., and Seckl, J. R. (2004) Novel adipose tissue-mediated resistance to diet-induced visceral obesity in 11β-hydroxysteroid dehydrogenase type 1-deficient mice. *Diabetes* **53,** 931–938
13. Wamil, M., Battle, J. H., Turban, S., Kipari, T., Seguret, D., de Sousa Peixoto, R., Nelson, Y. B., Nowakowska, D., Ferenbach, D., Ramage, L., Chapman, K. E., Hughes, J., Dunbar, D. R., Seckl, J. R., Morton, N. M. (2011) Novel fat depot-specific mechanisms underlie resistance to visceral obesity and inflammation in 11β-hydroxysteroid dehydrogenase type 1-deficient mice. *Diabetes* **60,** 1158–1167
14. Small, G. R., Hadoke, P. W., Sharif, I., Dover, A. R., Armour, D., Kenyon, C. J., Gray, G. A., Walker, B. R. (2005) Preventing local regeneration of glucocorticoids by 11β-hydroxysteroid dehydrogenase type 1 enhances angiogenesis. *Proc. Natl. Acad. Sci. U.S.A.* **102,** 12165–12170
15. McSweeney, S. J., Hadoke, P. W., Kozak, A. M, Small, G. R., Khaled, H., Walker, B. R., Gray, G. A. (2010) Improved heart function follows enhanced inflammatory cell recruitment and angiogenesis in 11βHSD1-deficient mice post-MI. *Cardiovasc Res.* **88,** 159–167
16. Maxwell, P. H., Wiesener, M. S., Chang, G. W., Clifford, S. C., Vaux, E. C., Cockman, M. E., Wykoff, C. C., Pugh, C. W., Maher, E. R., and Ratcliffe, P. J. (1999) The tumor suppressor protein VHL targets hypoxia-inducible factors for oxygen-dependent proteolysis. *Nature* **399,** 271–275
17. Epstein, A. C., Gleadle, J. M., McNeill, L. A., Hewitson, K. S., O'Rourke, J., Mole, D. R., Mukherji, M., Metzen, E., Wilson, M. I., Dhanda, A., Tian, Y. M., Masson, N., Hamilton, D. L., Jaakkola, P., Barstead, R., Hodgkin, J., Maxwell, P. H., Pugh, C. W., Schofield, C. J., and Ratcliffe, P. J. (2001) *Caenorhabditis elegans* EGL-9 and mammalian homologs define a family of dioxygenases that regulate HIF by prolyl hydroxylation. *Cell* **107,** 43–54
18. Ivan, M., Kondo, K., Yang, H., Kim, W., Valiando, J., Ohh, M., Salic, A., Asara, J. M., Lane, W. S., and Kaelin, W. G., Jr. (2001) HIFα targeted for VHL-mediated destruction by proline hydroxylation: implications for O_2 sensing. *Science* **292,** 464–468
19. Copple, B. L., Bai, S., Moon, J. O. (2010) Hypoxia-inducible factor-dependent production of profibrotic mediators by hypoxic Kupffer cells. *Hepatol. Res.* **40,** 530–539
20. Iredale, J. P. (2007) Models of liver fibrosis: exploring the dynamic nature of inflammation and repair in a solid organ. *J. Clin. invest.* **117,** 539–548
21. Eickelberg, O. (2001) Endless healing: TGF-β, SMADs, and fibrosis. *FEBS Lett.* **506,** 11–14
22. Keophiphath, M., Achard, V., Henegar, C., Rouault, C., Clément, K., and Lacasa, D. (2009) Macrophage-secreted factors promote a profibrotic

phenotype in human preadipocytes. *Mol. Endocrinol.* **23,** 11–24
23. Friedman, S. L. (2010) Evolving challenges in hepatic fibrosis. *Nat. Rev. Gastroenterol. Hepatol.* **7,** 425–436
24. Stockmann, C., Kerdiles, Y., Nomaksteinsky, M., Weidemann, A., Takeda, N., Doedens, A., Torres-Collado, A. X., Iruela-Arispe, L., Nizet, V., and Johnson, R. S. (2010) Loss of myeloid cell-derived vascular endothelial growth factor accelerates fibrosis. *Proc. Natl. Acad. Sci. U.S.A.* **107,** 4329–4334
25. Gealekman, O., Burkart, A., Chouinard, M., Nicoloro, S. M., Straubhaar, J., and Corvera, S. (2008) Enhanced angiogenesis in obesity and in response to PPARγ activators through adipocyte VEGF and ANGPTL4 production. *Am. J. Physiol. Endocrinol. Metab.* **295,** E1056–E1064
26. Arany, Z., Foo, S. Y., Ma, Y., Ruas, J. L., Bommi-Reddy, A., Girnun, G., Cooper, M., Laznik, D., Chinsomboon, J., Rangwala, S. M., Baek, K. H., Rosenzweig, A., and Spiegelman, B. M. (2008) HIF-independent regulation of VEGF and angiogenesis by the transcriptional coactivator PGC-1α. *Nature* **451,** 1008–1012
27. Ndubuizu, O. I., Tsipis, C. P., Li, A., LaManna, J. C. (2010) Hypoxia-inducible factor-1 (HIF-1)-independent microvascular angiogenesis in the aged rat brain. *Brain Res.* **1366,** 101–109
28. Nauck, M., Karakiulakis, G., Perruchoud, A. P., Papakonstantinou, E., Roth, M. (1998) Corticosteroids inhibit the expression of the vascular endothelial growth factor gene in human vascular smooth muscle cells. *Eur. J. Pharmacol.* **341,** 309–315
29. Leonard, M. O., Godson, C., Brady, H. R., Taylor, C. T. (2005) Potentiation of glucocorticoid activity in hypoxia through induction of the glucocorticoid receptor. *J. Immunol.* **174,** 2250–2257
30. De Sousa Peixoto, R. A., Turban, S., Battle, J. H., Chapman, K. E., Seckl, J. R., Morton, N. M. (2008) Preadipocyte 11β-hydroxysteroid dehydrogenase type 1 is a keto-reductase and contributes to diet-induced visceral obesity *in vivo*. *Endocrinology* **149,** 1861–1868
31. Villaret, A., Galitzky, J., Decaunes, P., Estève, D., Marques, M. A., Sengenès, C., Chiotasso, P., Tchkonia, T., Lafontan, M., Kirkland, J. L., Bouloumié, A. (2010) Adipose tissue endothelial cells from obese human subjects: differences among depots in angiogenic, metabolic, and inflammatory gene expression and cellular senescence. *Diabetes* **59,** 2755–2763
32. Ye, J., Gao, Z., Yin, J., and He, Q. (2007) Hypoxia is a potential risk factor for chronic inflammation and adiponectin reduction in adipose tissue of *ob*/*ob* and dietary obese mice. *Am. J. Physiol. Endocrinol. Metab.* **293,** E1118–E1128
33. Kodama, T., Shimizu, N., Yoshikawa, N., Makino, Y., Ouchida, R., Okamoto, K., Hisada, T., Nakamura, H., Morimoto, C., and Tanaka, H. (2003) Role of the glucocorticoid receptor for regulation of hypoxia-dependent gene expression. *J. Biol. Chem.* **278,** 33384–33391
34. Haddad, J. J., Land, S. C. (2001) A non-hypoxic, ROS-sensitive pathway mediates TNF-α-dependent regulation of HIF-1α. *FEBS Lett.* **505,** 269–274
35. Jung, Y. J., Isaacs, J. S., Lee, S., Trepel, J., Neckers, L. (2003) IL-1β-mediated up-regulation of HIF-1α via an NFκB/COX-2 pathway identifies HIF-1 as a critical link between inflammation and oncogenesis. *FASEB J.* **17,** 2115–2117
36. Feldser, D., Agani, F., Iyer, N. V., Pak, B., Ferreira, G., and Semenza, G. L (1999) Reciprocal positive regulation of hypoxia-inducible factor 1α and insulin-like growth factor 2. *Cancer Res.* **59,** 3915–3918
37. Treins, C., Giorgetti-Peraldi, S., Murdaca, J., Semenza, G. L., Van Obberghen, E. (2002) Insulin stimulates hypoxia-inducible factor 1 through a phosphatidylinositol 3-kinase/target of rapamycin-dependent signaling pathway. *J. Biol. Chem.* **277,** 27975–27981
38. He, Q., Gao, Z., Yin, J., Zhang, J., Yun, Z., Ye, J. (2011) Regulation of HIF-1α activity in adipose tissue by obesity-associated factors: adipogenesis, insulin, and hypoxia. *Am. J. Physiol. Endocrinol. Metab.* **300,** E877–885